THE JOURNAL OF PHYSICAL CHEMISTRY Letters

Letter

pubs.acs.org/JPCL

Insight into Enhanced Cycling Performance of Li−O_2 Batteries Based on Binary $CoSe_2$/CoO Nanocomposite Electrodes

Shanmu Dong,[†] Shan Wang,[†] Jing Guan,[†] Shanming Li,[‡] Zhenggang Lan,[†] Chun Chen,[§] Chaoqun Shang,[†] Lixue Zhang,[†] Xiaogang Wang,[†] Lin Gu,*[,‡] Guanglei Cui,*[,†] and Liquan Chen[‡]

[†]Qingdao Key Lab of Solar Energy Utilization and Energy Storage Technology, Qingdao Institute of Bioenergy and Bioprocess Technology, Chinese Academy of Sciences, Qingdao 266101, People's Republic of China

[‡]Institute of Physics, Chinese Academy of Sciences, Beijing 100090, People's Republic of China

[§]Department of Chemistry, Beijing Institute of Technology, Bejing 102488, People's Republic of China

Supporting Information

ABSTRACT: In this study, binary core−shell $CoSe_2$/CoO nanocomposites are synthesized as cathodic electrodes for the Li−O_2 cell, which exhibits enhanced cycle performance. From theoretical calculations, aberration-corrected scanning transmission electron microscopy observation, and gas chromatography mass spectrum verification, we propose that an enhanced cycle performance can be attributed to the improvement of the compatibility of the cathode/Li_2O_2 interface, which results from preferable interaction between Li_2O_2 intermediates and the CoO "shell" and then reduction of interfacial Li_2CO_3 formation on the carbon surface. Furthermore, our findings demonstrate that the $CoSe_2$ "core" may impact the electronic structure of surface metal ions, generating a superior cycling performance than that of pristine CoO materials. These results will offer some critical insights into the mechanistic process of Li−O_2 batteries.

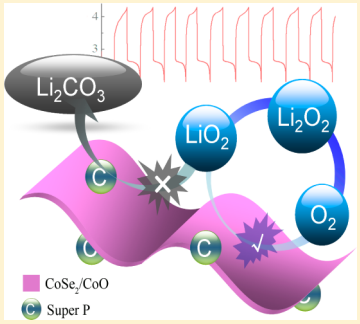

SECTION: Energy Conversion and Storage; Energy and Charge Transport

The lithium−air battery, which has a theoretical energy density comparable with that of gasoline, has been considered one of the most promising energy storage devices for electric vehicles.[1−3] However, high overpotential and short cycle life pose ever-increasing challenges to the currently investigated Li−O_2 cell.[2−6] Since the cell failure originating from electrolyte decomposition and consequently cathode interfacial passivation has been demonstrated by several groups,[7−10] substantial research has been carried out to find a more stable electrolyte.[11−13] Although the desirable discharge product Li_2O_2 has been detected in these electrolytes, the problem of limited cycle life remains unsolved.[14,15] As pointed out by P. G Bruce et al., the enhanced lifespan of Li−O_2 batteries relies on the synergy of the electrolyte, discharge products, and cathodic electrode rather than each in isolation.[16] Consequently, the exploration of a cathode with a favorable interface toward electrolyte and discharge products is also of extreme importance to enhance the overall cycle performance.

Recently, the investigation of the electrocatalytic role of a cathodic electrode in the oxygen evolution reaction (OER) in a nonaqueous system has raised controversial arguments. Several authors have reported electrocatalysts exhibiting an excellent property in catalyzing the Li_2O_2 decomposition and lowering the overpotential,[17−20] while, according to Luntz et al., the reduced overpotential is indicative of the electrocatalysis related to electrolyte decomposition and that a conventional electrocatalyst may be implausible.[21,22] To bridge the two schools of thoughts, two recent studies offered possible explanations. Yang et al. suggested that the OER occurs in two distinct stages during the charging process.[23] The first stage at low overpotential with a sloping voltage profile is relatively insensitive to catalysts, while the second stage at high overpotential is lowered significantly with the presence of catalysts. The study by Nazar et al. reported a similar charging process.[24] In their work, Co_3O_4/RGO was considered as a so-called "promoter" to change interfacial transport of Li_xO_2 species on cathode materials, rather than as a conventional electrocatalyst to lower the activation energy through electron transfer. However, it is a challenge to provide convincing proof to explain how Co_3O_4 modifies the interfacial transport of Li_2O_2 intermediates. Therefore, further studies are required to elucidate the reaction taking place on the cathode/Li_2O_2 interface during the charge and discharge process. Furthermore, after 20 cycles, the enhanced cycle performance is overwhelmed by the deposition of side products, which suggests that Co_3O_4 may not be the optimal material to enhance the cycling stability. Nowadays, Co_3O_4 has been widely investigated for Li−O_2 battery cathodes,[24−26] while other chalcogenide materials with a similar electronic structure, such as sulfide and selenide, are rarely explored and could also be expected to deliver better performance.

Received: December 21, 2013
Accepted: January 21, 2014
Published: January 21, 2014

Herein, we report an enhanced cycle performance of a Li−O_2 battery based on a binary core−shell $CoSe_2$/CoO nanocomposite (CSCO) electrode obtained from a cobalt selenide nanobelt. Aberration-corrected scanning transmission electron microscopy (STEM) is involved to visually characterize the presence of O vacancies on the surface of a CoO shell. In combination with theoretical calculations, our findings suggest that the surface of this nanocomposite may deliver favorable sites for the chemical adsorption of Li_2O_2 intermediates and consequently reduce the accumulation of Li_2CO_3 on carbon materials. This study demonstrates a novel Co-based binary nanocomposite cathode with enhanced interfacial stability and provides new insights into the mechanism of Li−O_2 batteries with enhanced cycling performance.

The binary CSCO was synthesized through in situ oxidation of a cobalt selenide nanobelt, which provided a firm contact of the two compounds.[27] By investigating the rechargeability of CSCO with various proportions of Se/O, the optimized annealing time was determined as 4 h. Figure 1a exhibits the X-ray diffraction (XRD) pattern of the nanocomposite. The reflections index to a mixture of the cubic $CoSe_2$ phase (JCPDS 65-3327) and the cubic rocksalt CoO phase (JCPDS 43-1004), suggesting the formation of a binary nanocomposite. Transmission electron microscopy (TEM) images (Figure 1b) reveal that the CSCO partly maintained the nanobelt morphology of the cobalt selenide precursor (See Figure S1, Supporting Information), while some shrinkage of the smooth surface arising from lattice structure recrystallization was also observed. An image of high-resolution transmission electron microscopy (HRTEM) in Figure 1c displays core/shell structures with the $CoSe_2$ core nearly fully wrapped by coating the CoO layer. EDX mapping results further confirm this core−shell structure (see Figure S2, Supporting Information). However, the partial oxidation of $CoSe_2$ results in a nonuniform morphology of the shell layer. The observed and calculated *d*-spacings from regions A and B are 0.340 and 0.148 nm, which matches well with the *d*-spacing of {111} facets of CoO and {210} facets of $CoSe_2$, respectively.

O vacancies on the surface of electrode materials are critical to the reaction of oxygen electrocatalysis.[28,29] However, there are still limited reports visually illustrating O vacancies of the cathode for the Li−O_2 cell at atomic resolution through aberration-corrected STEM. As shown in the annular bright-field micrographs of the CoO shell, the long-range order of the CoO crystal is destroyed by the edge of the surface, which is considered as surface reconstructions driven by suboxides (Figure 1d,e). Further evidence is displayed in the line profile along the [100] axis; the O vacancy concentration gradually increases from the inner to outer surface (Figure 1f,g). According to Nazar et al., the oxygen vacancies on the oxides can serve as an active center for binding the Li_2O_2 intermediates and thus facilitating the charging process.[30] The results in this study visually demonstrated the presence of O vacancies on the surface of CSCO, which may contribute to a favorable interface for the cathode reaction process.

To investigate the electrochemical performance, the O_2 electrode were prepared by mixing the CSCO with 40% Super P (SP) and 10% binder. The 1 M LiTFSI/triethylene glycol dimethyl ether (TEGDME) was employed as an electrolyte. A lithium metal anode, a glass fiber separator, and the binary nanocomposite cathode were assembled into Swagelok cells. Figure 2a depicts the galvanostatic charge−discharge curves of the $CoSe_2$/CoO/SP (CSCO/SP) electrode.

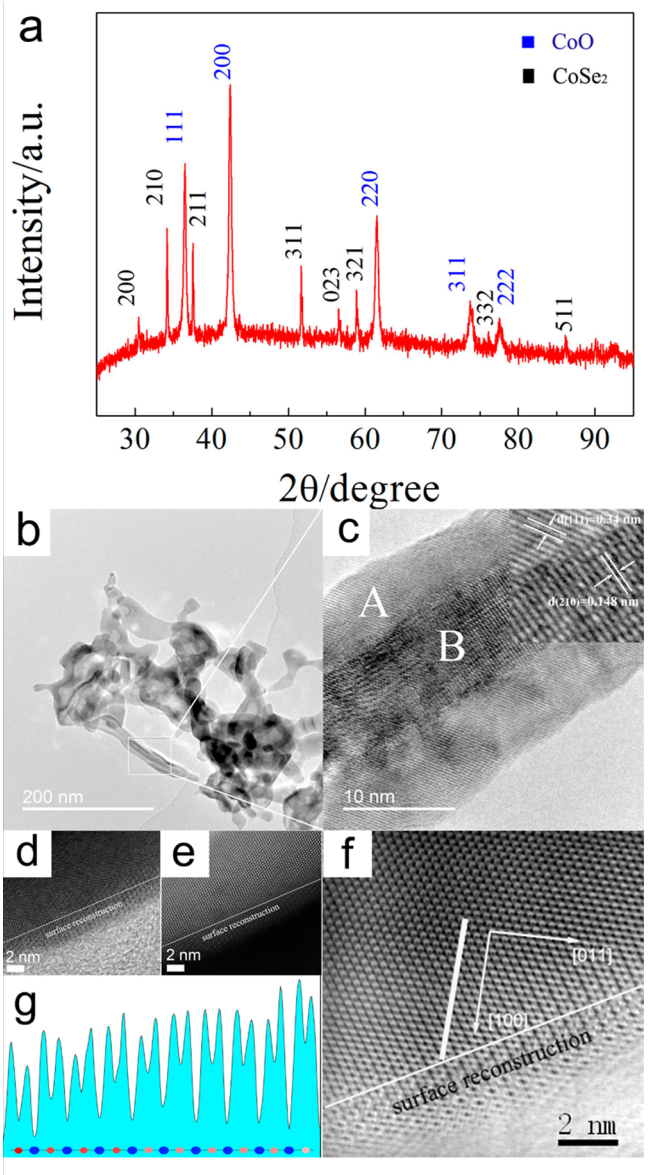

Figure 1. (a) XRD pattern of the as-prepared binary Co-based chalcogenide nanocomposites; TEM (b) and HRTEM (c) images of CSCO. Regions A and B indicate the shell of CoO and the core of $CoSe_2$ as the *d*-spacings matched well with those of {111} facets of CoO and {210} facets of $CoSe_2$, respectively. Aberration-corrected STEM images of CSCO; (d) annular bright-field and (e) corresponding high-angle annular dark-field images of the CoO shell layer. (f) The white line indicates where the line profile is located, and the direction of the line profile is taken along the [100] direction. (g) The line profile along the Co−O−Co chains in (f). The blue and red circles indicate Co and O ions, respectively. The lighter red circle indicates the presence of oxygen vacancies.

In the first cycle, a discharge capacity of about 1500 mA h g^{-1} could be delivered with a plateau between 2.7 and 2.6 V at a current density of 0.1 mA cm^{-2}. This capacity seems to be moderate compared with those in recent studies. However, high capacities reported in recent studies were always obtained with low loading amount (less than 1 mg/cm^2 and some of them even lower than 0.5 mg/cm^2), which are less than 25% of that in our studies (4 mg/cm^2). XRD patterns (Figure 2b) of the discharged electrode demonstrate the formation of Li_2O_2. Furthermore, toroid-shaped particles were found on the

dx.doi.org/10.1021/jz402755b | J. Phys. Chem. Lett. 2014, 5, 615−621

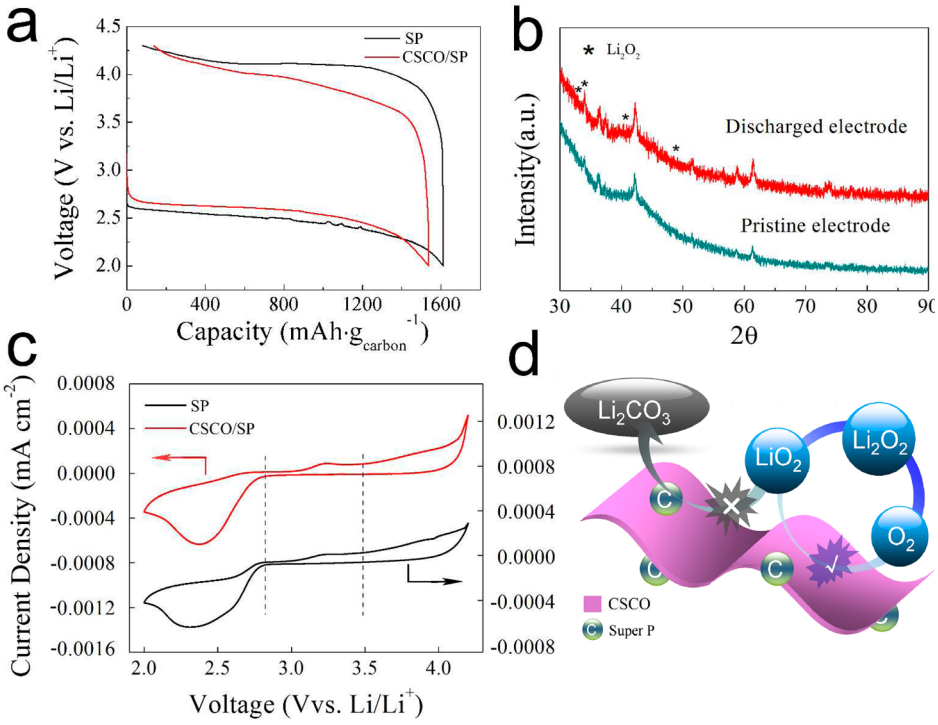

Figure 2. (a) The first cycle discharge−charge profiles of SP (black) and CSCO/SP (red) electrodes at a current density of 0.1 mA/cm^2. (b) XRD patterns of the pristine CSCO/SP electrodes (blue) and after first discharge (red). Reflections of Li_2O_2 are marked. (c) CV curves of SP (black) and CSCO/SP (red) at a scan rate of 0.5 mV s^{-1}. (d) Schematic illustration of the proposed CSCO/SP reaction mechanism in Li−O_2 batteries. The CSCO may offer a favorable site for the chemical adsorption of Li_2O_2 intermediates during the charging process and limit the contact of Li_2O_2 intermediates with carbon materials, which facilitates the cycle of Li_2O_2 reversible decomposition and limits the accumulation of Li_2CO_3 caused by carbon oxidation.

electrode surface, which are recognized as typically shaped of Li_2O_2 (see Figure S3, Supporting Information). It should be noted that the discharge profile of CSCO/SP is similar to that of the SP cathode (based on the mass of carbon), indicating a comparable electrocatalytic activity of both cathodes toward O_2 reduction. Cycle voltammetry (CV) curves in Figure 2c also confirm this finding. During the charging process, the CSCO distinctly impacts the O_2 OER in galvanostatic charge−discharge analysis as the CSCO/SP electrode exhibits a lower charge plateau than that of the SP electrode. On the other hand, the onset potential in CV for recharging is similar for both cathodes. These results are in accordance with the findings reported by Nazar et al.[24] However, up to now, it is still a challenge to confirm the exact location of Li_2O_2 on the cathode surface (see Figure S4a, Supporting Information).

To approach the possible mechanism for the OER catalytic activity of CSCO, the recent study on carbon cathode (Bruce et al.) may offer major implications.[16] According to their report, during the charging process, carbon materials decompose to form Li_2CO_3 arising from a reaction involving the intermediate of Li_2O_2, which is generally proposed as LiO_2.[16,23,31−33] Because the superoxide is a strong nucleophile, hydrophilic carbon with a more polar surface (such as C−O, COOH) is more reactive for nucleophilic attack. These results inspire us to theoretically investigate the interfacial stability of the CSCO/SP electrode. Using the density functional theory (DFT) method, the chemical adsorption of the superoxide on the surface of carbon materials and binary Co-based nanocomposites is investigated. Because CoO exists in the shell of the CSCO, the analysis of LiO_2 surface adsorption behavior is carried out by calculating the optimum adsorption mode and strength of interaction of LiO_2 onto CoO and an SP surface. We calculate the optimum adsorption mode and strength of interaction of LiO_2 onto various cobalt oxide surfaces, including Co−CoO(111), O−CoO(111), CoO(100), and CoO(110). As demonstrated in Figure 3, the adsorption of molecular LiO_2 follows some general patterns, in which LiO_2 oxygen atoms interact with surface Co cations and the Li atom interacts with surface basic O^{2-} sites. On the basis of our DFT calculations, it is observed that the exothermicity for LiO_2 adsorption on various surfaces increases in the order of Co−CoO(111) >

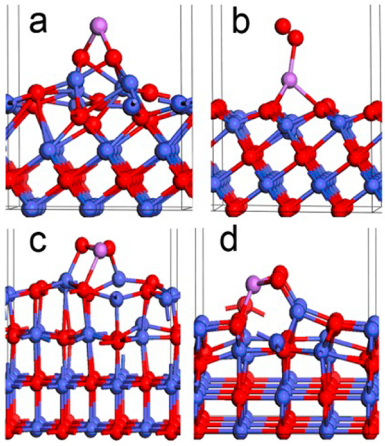

Figure 3. Side views of the most stable adsorption configurations of LiO_2 on Co--CoO(111) (a), O−CoO (111) (b), CoO(100) (c), and CoO(110) (d) surfaces.

dx.doi.org/10.1021/jz402755b | J. Phys. Chem. Lett. 2014, 5, 615−621

CoO(110) > CoO(100) > O−CoO(111) (detailed information of the computational calculations is shown in the Supporting Information section S6.3). The Super P carbon black is comprised of a chain-like structure of interconnected carbon particles. Within each particle, a carbon-like nanostructure composed mainly of sp^2-hybridized carbon atoms is observed. In this study, the graphite model is used to mimic the frameworks of Super P carbon black and systematically investigate the adsorption of LiO_2 onto the Super P surface. To demonstrate the high selectivity of cobalt oxide for LiO_2 adsorption, the adsorption energies of LiO_2 on both pristine and OH-functionalized graphite sheets are calculated and compared with the adsorption of LiO_2 on these cobalt oxides (see Figure S7, Supporting Information). We found that the binding energy of LiO_2 onto the CoO surface (−2.7 to −13.4 eV) is significantly higher than the corresponding value for carbon materials (0.1 to −0.3 eV). Furthermore, the O vacancies on the surface of CoO (illustrated in Figure 1d−g) may also serve as the binding center for superoxide.[29,30] These results of theoretical calculation and experimental observation make us believe that LiO_2 may tend to bind with the CSCO compared to the carbon material (this supposition is different from previous reports by Nazar et al., which regard carbon as a more "sticky" material for superoxide than metal oxide[24]). Therefore, a more stable interface is obtained on the CSCO/SP cathode as carbon materials can be protected from being preferentially oxidized by the strong nucleophilic superoxide, and thus, the interfacial formation of Li_2CO_3 by carbon decomposition can be limited (as shown in Figure 2d). Because the Li_2CO_3 layer on the cathode surface enhances the interfacial resistance,[34,35] the presence of CSCO decreasing the amount of Li_2CO_3 can lower the overpotential during galvanostatic charging. To further demonstrate this proposal, GC-MS analyses were performed to measure the composition of the gas released at the end of the first charging cycle. Compared with the SP electrode, the presence of CSCO lowers the proportion of CO_2 that is produced by Li_2CO_3 and electrolyte decomposition with a potential above 4 V (Table 1).[23,24,36]

Table 1. Analysis of Gas Products after First Charge Using GC-MS for Li−O_2 Batteries Based on CSCO/SP and SP Cathodes

	O_2 (%)	CO_2 (%)	O_2/CO_2
SP	14.40	0.64	22.5
CSCO/SP	13.84	0.23	60.2

Although the side reaction of the electrolyte and LiO_2 cannot be excluded,[34] this result further indicates that CSCO/SP can provided a more stable interface by reducing the accumulation of Li_2CO_3 from carbon oxidization during the charge process.

According to Luntz et al., even only a layer of Li_2CO_3 accumulated on the cathode interface results in an augment of potential during the charging process and consequential electrolyte stability issues, which finally lead to cycle degradation.[34] Therefore, a better cycling of Li_2O_2 for CSCO/SP electrodes can be expected by lowering the amount of Li_2CO_3 at the carbon interface. Figure 4a displays charge/discharge profiles of CSCO/SP electrodes for 30 cycles. Although a gradual fading of capacity was observed, the capacity retention of ∼50% for 30 cycles still represented a notable enhancement over SP cathodes (sharp capacity fading with less than 30% retention for 5 cycles). This result is

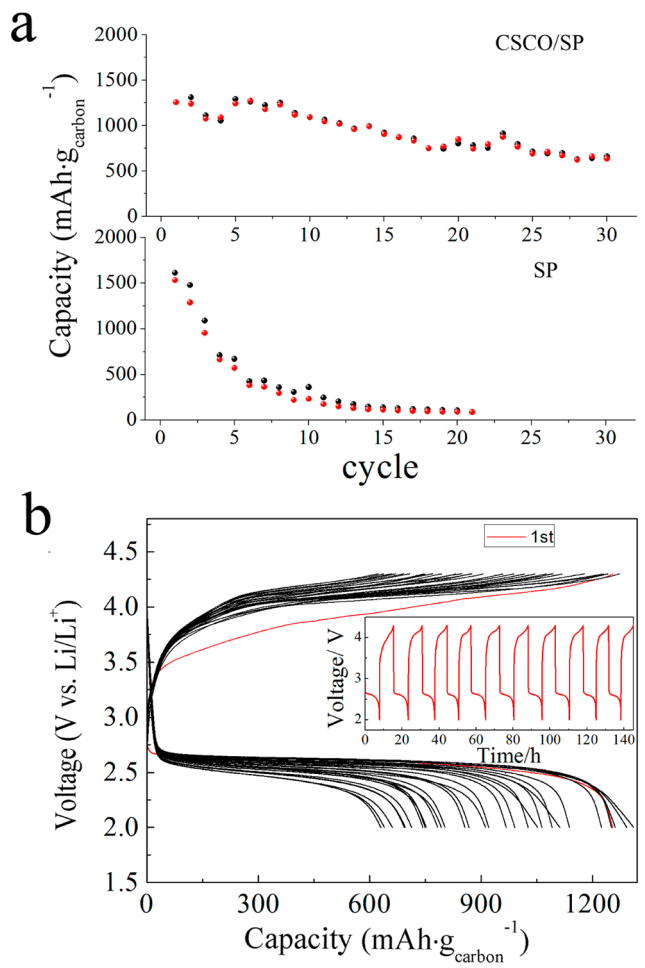

Figure 4. (a) The cycle performance of the SP cathode and CSCO/SP. (b) discharge/charge profiles of the Li−O_2 cell with CSCO/SP for 30 cycles at a current rate of 0.1 mA/cm^2. (Inset) Voltage−time curves of the initial 10 cycles.

consistent with our supposition that CSCO offers favorable sites for the binding of LiO_2 species and reduces the amount of Li_2CO_3 formed by carbon decomposition. Although the cycle number of this Li−O_2 cell is still limited, two aspects of the improved cycle performance deserve special highlights. First, a high Coulombic efficiency during cycles is achieved by CSCO/SP, demonstrating a stable formation/decomposition cycling process. Second, cycling was done with a deep discharge to 2 V under no restriction of charge/discharge capacity. Compared with recent studies displaying the cycling performance under no restriction of capacity, this CSCO-based Li−O_2 cell exhibited superior cycling ability.[37−44] The high cycle numbers reported in recent studies are generally obtained by restricting the capacity. The restricted capacity is generally less than 50% of the total capacity (capacity discharged to 2 or 2.2 V). Therefore, with a low loading amount of electrode, these cycling tests can be completed in a very short period. In our case, the cycling tests were discharged to 2 V with no restricting capacity. As shown in Figure 4b, 10 cycles last for more than 140 h, which is comparable with that of some recent studies for 100 cycles.

The results displayed in Figure 5a indicate that the $CoSe_2$ "core" inside of the nanocomposites also impacts the interfacial stability, resulting in a superior overall cycleability. As shown in the electron energy-loss spectroscopy (EELS) spectra, the L_3/

dx.doi.org/10.1021/jz402755b | J. Phys. Chem. Lett. 2014, 5, 615−621

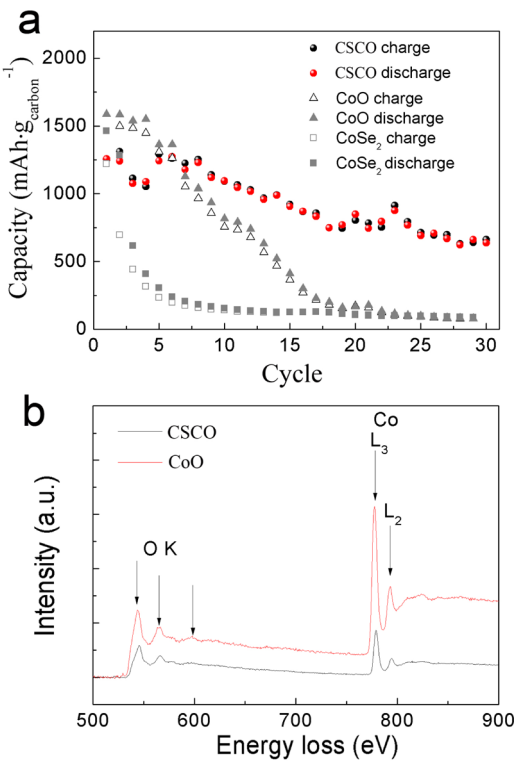

Figure 5. (a) The cycle performance of CoO-, $CoSe_2$-, and CSCO-based cathodes. (b) The EELS spectra of CoO and CSCO materials.

L_2 intensity ratios of Co are 1.947 and 2.438 for CoO and $CoSe_2$/CoO, respectively. This clear difference demonstrates a variation of the valence state of surface Co ions. Because the partial oxidation of $CoSe_2$ results in a nonuniform shell layer of CoO, the shell of CoO can be very thin at certain sites. Therefore, the electron may transfer from $CoSe_2$ to CoO, modifying the electronic structure of surface metal ions. This unique electronic structure of CSCO may offer a more favorable interface for the chemical adsorption of the intermediate of Li_2O_2 than that of simply CoO materials, reducing the accumulation of Li_2CO_3 on carbon materials and hence improving the cycle performance. Our findings indicate that the optimization of the electronic structure of surface transition-metal ions is definitely important for enhancing the interface stability and improving cycle performance of the chalcogenide-based electrode in the Li–O_2 cell.

In summary, a binary $CoSe_2$/CoO core–shell nanocomposite-based electrode significantly improves the cycle performance of Li–O_2 batteries, which leads to some insights into cathode processes. It is proposed that this nanocomposite might provide a more compatible interface by facilitating the chemical adsorption of Li_2O_2 intermediates. Corroborated by DFT computation, a more favorable interaction of LiO_2 with CoO than that with carbon material is demonstrated. The O vacancies are confirmed on the surface of CoO through an aberration-corrected STEM, which may also serve as the active sites for the binding of superoxide. Moreover, GC-MS analysis at the end of the charge process shows that the presence of CSCO lowers the proportion of CO_2, suggesting a reduction of the accumulation of Li_2CO_3. Owing to the "core" of $CoSe_2$ materials impacting the valence state of surface Co ions, CSCO-based electrodes deliver more stable interfaces and superior cycle performance than simply CoO materials. On the basis of these investigations, we suggested that the optimization of the surface electronic structure of Co-based oxides is of vital importance for constructing a cathode reaction interface with good reversibility and cycleability. These insights will provide some implications for further fundamental research on the charging reaction process of Li–O_2 batteries.

EXPERIMENTAL SECTION

Synthesis of $CoSe_2$/CoO Composites. The synthesis scheme for CSCO involved a solvothermal synthesis of cobalt selenide nanobelts and subsequent oxidation. Cobalt selenide/diethylenetriamine (DETA) nanobelts were synthesized first by a solvothermal strategy reported by Shu-Hong Yu et al.[27] Na_2SeO_3 and $Co(Ac)_2{\cdot}4H_2O$ were used as reactants, and a mixed solution of DETA and deionzed water was used as the reaction solvent. During the heating process, DETA molecules were protonated by the water and then acted as a template to induce the growth of a 1D nanostructure (as evidenced by the SEM images Figure S1, Supporting Information). The CSCO's were obtained by treating the cobalt selenide nanobelts at 450 °C for 4 h under flowing 0.1% O_2 containing a high-purity Ar atmosphere. For comparison, $CoSe_2$ and CoO were synthesized by the same procedure but annealed under 100% Ar and 1% O_2 + 99% Ar, accordingly.

Physical Characterization. The XRD pattern was recorded on a Bruker-AXS Microdiffractometer (D8 ADVANCE) from 10 to 85°. Morphological and structural information were obtained from scanning electron microscopy (SEM) (HITACHI S-4800) and high-resolution transmission electron microscopy (HRTEM, JEOL 2010F). Scanning transmission electron microscopy (STEM) was performed on a ARM 200F transmission electron microscope (JEOL; double spherical aberration correction) operating at 200 kV. STEM images were recorded with a high-angle annular dark-field (HAADF) detector (70–250 mrad) and an annular bright-field (ABF) detector (12–25 mrad). Electron energy-loss spectroscopy (EELS) was acquired using a Gatan Imaging Filter system attached to a Tecnai F20 microscope.

Li–O_2 Cell Assembly and Tests. The cathodic electrodes (typically 1.0 mg) were prepared by mixing 50 wt % $CoSe_2$/CoO with 40 wt % SP and 10 wt % polytetrafluoroethlyene (PTFE) binders or 90 wt % SP with 10 wt % PTFE. The samples were rolled into slices and cut into square pieces of 0.5 cm × 0.5 cm and then pasted on a stainless steel current collector under a pressure of 5 MPa. Electrochemical experiments were carried out by using a swagelok cell with a hole drilled only on the cathode of the current collector to enable oxygen flow in. The Li–O_2 cells were assembled inside of the glovebox under an argon atmosphere (<1 ppm H_2O and O_2) by using a clean lithium metal disk (8 mm diameter) as the anode, a glass fiber and polypropylene (Celgard 2400) as separators, and 1 M LiTFSI in TEGDME as the electrolyte. Galvanostatical discharge–charge experiments were tested in a LAND battery testing system. For the analysis of gaseous products generated during the charging step, as described by Liu et al.,[19] the test cells were first discharged in an O_2 atmosphere, and then, the oxygen was completely flushed out by ultrahigh-purity Ar. A gas sample was taken from the cell to make a baseline before the charging process. Gas samples for the background analysis and produced during the charging step were analyzed by gas chromatography mass spectrometry (GC-MS, ITQ1100, Thermo Fisher).

dx.doi.org/10.1021/jz402755b | J. Phys. Chem. Lett. 2014, 5, 615–621

Theoretical Calculations. Density functional theory (DFT) calculations were performed using the Vienna ab initio simulation package (VASP). Computational details are provided in the Supporting Information.

■ ASSOCIATED CONTENT

Supporting Information

SEM image of $CoSe_2$/DETA, SEM image of the electrode after discharging, and computational details. This material is available free of charge via the Internet at http://pubs.acs.org.

■ AUTHOR INFORMATION

Corresponding Authors

*E-mail: cuigl@qibebt.ac.cn. Tel: (+86) 532-80662746. Fax: (+86) 532-80662744 (G.C.).

*E-mail: l.gu@iphy.ac.cn. Tel: (+86) 532-80662746. Fax: (+86) 532-80662744 (L.G.).

Notes

The authors declare no competing financial interest.

■ ACKNOWLEDGMENTS

This work was supported by the Key Research Program of the Chinese Academy of Sciences (Grant No. KGZD-EW-202-2), the National Natural Science Foundation of China (Grant No. 21275151, 21271180, 21301185), the National High Technology Research and Development Program of China (863 Program, No. 2013AA050905), the National Program on Key Basic Research Project of China (No. MOST2011CB935700), the State Key Laboratory of Electroanalytical Chemistry (No. SKLEAC201302), and the Key Technology Research Projects of Qingdao (No. 12-4-1-24-gx).

■ REFERENCES

(1) Abraham, K. M.; Jiang, Z. Polymer Electrolyte-Based Rechargeable Lithium/Oxygen Battery. *J. Electrochem. Soc.* **1996**, *143*, 1−5.

(2) Debart, A.; Paterson, A. J.; Bao, J.; Bruce, P. G. α-MnO_2 Nanowires: A Catalyst for the O_2 Electrode in Rechargeable Lithium Batteries. *Angew. Chem., Int. Ed.* **2008**, *47*, 4521−4524.

(3) Girishkumar, G.; McCloskey, B.; Luntz, A. C.; Swanson, S.; Wilcke, W. Lithium−Air Battery: Promise and Challenges. *J. Phys. Chem. Lett.* **2010**, *1*, 2193−2203.

(4) Shao, Y.; Ding, F.; Xiao, J.; Zhang, J.; Xu, W.; Park, S.; Zhang, J.-G.; Wang, Y.; Liu, J. Making Li−Air Batteries Rechargeable: Material Challenges. *Adv. Funct. Mater.* **2013**, *23*, 987−1004.

(5) Lu, Y.-C.; Gallant, B. M.; Kwabi, D. G.; Harding, J. R.; Mitchell, R. R.; Whittingham, M. S.; Yang, S.-H. Lithium−Oxygen Batteries: Bridging Mechanistic Understanding and Battery Performance. *Energy Environ. Sci.* **2013**, *6*, 750−768.

(6) McCloskey, B. D.; Bethune, D. S.; Shelby, R. M.; Mori, T.; Scheffler, R.; Speidel, A.; Sherwood, M.; Luntz, A. C. A. C. Limitations in Rechargeability of Li−O_2 Batteries and Possible Origins. *J. Phys. Chem. Lett.* **2012**, *3*, 3043−3047.

(7) Xu, W.; Xu, K.; Viswanathan, V. V.; Towne, S. A.; Hardy, J. S.; Xiao, J.; Nie, Z.; Hu, D.; Wang, D.; Zhang, J.-G. Reaction Mechanisms for the Limited Reversibility of Li−O_2 Chemistry in Organic Carbonate Electrolytes. *J. Power Sources* **2011**, *196*, 9631−9639.

(8) Freunberger, S. A.; Chen, Y.; Peng, Z.; Griffin, J. M.; Hardwick, L. J.; Barde, F.; Novak, P.; Bruce, P. G. Reactions in the Rechargeable Lithium−O_2 Battery with Alkyl Carbonate Electrolytes. *J. Am. Chem. Soc.* **2011**, *133*, 8040−8047.

(9) Laoire, C. O.; Mukerjee, S.; Abraham, K. M. Influence of Nonaqueous Solvents on the Electrochemistry of Oxygen in the Rechargeable Lithium−Air Battery. *J. Phys. Chem. C* **2010**, *114*, 9178−9186.

(10) Black, R.; Adams, B.; Nazar, L. F. Non-Aqueous and Hybrid Li−O_2 Batteries. *Adv. Energy Mater.* **2012**, *2*, 801−815.

(11) Peng, Z.; Freunberger, S. A.; Chen, Y.; Bruce, P. G. A Reversible and Higher-Rate Li−O_2 Battery. *Science* **2012**, *337*, 563−565.

(12) Zhang, T.; Zhou, H. A Reversible Long-Life Lithium−Air Battery in Ambient Air. *Nat. Commun.* **2013**, *4*, 1817.

(13) Hassoun, J.; Croce, F.; Armand, M.; Scrosati, B. Investigation of the O_2 Electrochemistry in a Polymer Electrolyte Solid-State Cell. *Angew. Chem., Int. Ed.* **2011**, *50*, 2999−3002.

(14) Laoire, C. Ó.; Mukerjee, S.; Plichta, E. J.; Hendrickson, M. A.; Abrahama, K. M. Rechargeable Lithium/TEGDME−$LiPF_6$/O_2 Battery. *J. Electrochem. Soc.* **2011**, *150*, A302−308.

(15) Freunberger, S. A.; Chen, Y.; Drewett, N. E.; Hardwick, L. J.; Barde, F.; Bruce, P. G. The Lithium−Oxygen Battery with Ether-Based Electrolytes. *Angew. Chem., Int. Ed.* **2011**, *50*, 8609−8613.

(16) Ottakam Thotiyl, M. M.; Freunberger, S. A.; Peng, Z.; Bruce, P. G. The Carbon Electrode in Nonaqueous Li−O_2 Cells. *J. Am. Chem. Soc.* **2013**, *135*, 494−500.

(17) Zhao, Y.; Xu, L.; Mai, L.; Han, C.; An, Q.; Xu, X.; Liu, X.; Zhang, Q. Hierarchical Mesoporous Perovskite $La_{0.5}Sr_{0.5}CoO_{2.91}$ Nanowires with Ultrahigh Capacity for Li−Air Batteries. *Proc. Natl. Acad. Sci. U.S.A.* **2012**, *109*, 19569−19574.

(18) Cao, Y.; Wei, Z.; He, J.; Zang, J.; Zhang, Q.; Zheng, M.; Dong, Q. α-MnO_2 Nanorods Grown In Situ on Graphene as Catalysts for Li−O_2 Batteries with Excellent Electrochemical Performance. *Energy Environ. Sci.* **2012**, *5*, 9765−9768.

(19) Shui, J.-L.; Karan, N. K.; Balasubramanian, M.; Li, S.-Y.; Liu, D.-J. Composite in Li−O_2 Battery: Studies of Catalytic Structure and Activity toward Oxygen Evolution Reaction. *J. Am. Chem. Soc.* **2012**, *134*, 16654−16661.

(20) Wu, G.; Mack, N. H.; Gao, W.; Ma, S.; Zhong, R.; Han, J.; Baldwin, J. K.; Zelenay, P. Nitrogen-Doped Graphene-Rich Catalysts Derived from Heteroatom Polymers for Oxygen Reduction in Nonaqueous Lithium−O_2 Battery Cathodes. *ACS Nano* **2012**, *6*, 9764−9776.

(21) McCloskey, B. D.; Scheffler, R.; Speidel, A.; Bethune, D. S.; Shelby, R. M.; Luntz, A. C. On the Efficacy of Electrocatalysis in Nonaqueous Li−O_2 Batteries. *J. Am. Chem. Soc.* **2011**, *133*, 18038−18041.

(22) McCloskey, B. D.; Scheffler, R.; Speidel, A.; Girishkumar, G.; Luntz, A. C. On the Mechanism of Nonaqueous Li−O_2 Electrochemistry on C and Its Kinetic Overpotentials: Some Implications for Li−Air Batteries. *J. Phys. Chem. C* **2012**, *116*, 23897−23905.

(23) Lu, Y.-C.; Yang, S.-H. Probing the Reaction Kinetics of the Charge Reactions of Nonaqueous Li−O_2 Batteries. *J. Phys. Chem. Lett.* **2013**, *4*, 93−99.

(24) Black, R.; Lee, J.-H.; Adams, B.; Mims, C. A.; Nazar, L. F. The Role of Catalysts and Peroxide Oxidation in Lithium−Oxygen Batteries. *Angew. Chem., Int. Ed.* **2012**, *51*, 1−6.

(25) Lim, H.-D.; Gwon, H.; Kima, H.; Kim, S.-W.; Yoon, T.; Choid, J. W.; Oh, S. M.; Kang, K. Mechanism of Co_3O_4/Graphene Catalytic Activity in Li−O_2 Batteries Using Carbonate Based Electrolytes. *Electrochim. Acta* **2013**, *90*, 63−70.

(26) Cui, Y.; Wen, Z.; Liu, Y. A Free-Standing-Type Design for Cathodes of Rechargeable Li−O_2 Batteries. *Energy Environ. Sci.* **2011**, *4*, 4727−4734.

(27) Gao, M.-R.; Yao, W.-T.; Yao, H.-B.; Yu, S.-H. Synthesis of Unique Ultrathin Lamellar Mesostructured $CoSe_2$−Amine (Protonated) Nanobelts in a Binary Solution. *J. Am. Chem. Soc.* **2009**, *131*, 7486−7487.

(28) Suntivich, J.; Gasteiger, H. A.; Yabuuchi, N.; Nakanishi, H.; Goodenough, J. B.; Yang, S.-H. Design Principles for Oxygen-Reduction Activity on Perovskite Oxide Catalysts for Fuel Cells and Metal−Air Batteries. *Nat. Chem.* **2011**, *3*, 546−550.

(29) Cheng, F.; Zhang, T.; Zhang, Y.; Du, J.; Han, X.; Chen, J. Enhancing Electrocatalytic Oxygen Reduction on MnO_2 with Vacancies. *Angew. Chem., Int. Ed.* **2013**, *52*, 1−5.

(30) Lee, J.-H.; Black, R.; Popov, G.; Pomerantseva, E.; Nan, F.; Botton, G. A.; Nazar, L. F. The Role of Vacancies and Defects in

$Na_{0.44}MnO_2$ Nanowire Catalysts for Lithium−Oxygen Batteries. *Energy Environ. Sci.* **2012**, *5*, 9558−9565.
(31) Adams, B. D.; Radtke, C.; Black, R.; Trudeau, M. L.; Zaghib, K.; Nazar, L. F. Current Density Dependence of Peroxide Formation in the Li−O_2 Battery and Its Effect on Charge. *Energy Environ. Sci.* **2013**, *6*, 1772−1778.
(32) Mo, Y.; Ong, S. P.; Ceder, G. First-Principles Study of the Oxygen Evolution Reaction of Lithium Peroxide in the Lithium−Air Battery. *Phys. Rev. B* **2011**, *84*, 205446.
(33) Gallant, B. M.; Kwabi, D. G.; Mitchell, R. R.; Zhou, J. Influence of Li_2O_2 Morphology on Oxygen Reduction and Evolution Kinetics in Li−O_2 Batteries. *Energy Environ. Sci.* **2013**, *6*, 2518−2528.
(34) McCloskey, B. D.; Speidel, A.; Scheffler, R.; Miller, D. C.; Viswanathan, V.; Hummelshøj, J. S.; Nørskov, J. K.; Luntz, A. C. Twin Problems of Interfacial Carbonate Formation in Nonaqueous Li−O_2 Batteries. *J. Phys. Chem. Lett.* **2012**, *3*, 997−1001.
(35) Gerbig, O.; Merkle, R.; Maier, J. Electron and Ion Transport In Li_2O_2. *Adv. Mater.* **2013**, *25*, 3129−3133.
(36) Lim, H.-K.; Lim, H.-D.; Park, K.-Y.; Seo, D.-H.; Gwon, H.; Hong, J.; Goddard, W. A.; Kim, H.; Kang, K. Toward a Lithium−"Air" Battery: The Effect of CO_2 on the Chemistry of a Lithium−Oxygen Cell. *J. Am. Chem. Soc.* **2013**, *135*, 9733−9742.
(37) Jung, H.-G.; Hassoun, J.; Park, J.-B.; Sun, Y.-K.; Scrosati, B. An Improved High-Performance Lithium−Air Battery. *Nat. Chem.* **2012**, *4*, 579−585.
(38) Li, F.; Zhang, T.; Yamada, Y.; Yamada, A.; Zhou, H. Enhanced Cycling Performance of Li−O_2 Batteries by the Optimized Electrolyte Concentration of LiTFSA in Glymes. *Adv. Energy Mater.* **2013**, *3*, 532−538.
(39) Jung, H.-G.; Jeong, Y. S.; Park, J.-B.; Sun, Y.-K.; Scrosati, B.; Lee, Y. J. Ruthenium-Based Electrocatalysts Supported on Reduced Graphene Oxide for Lithium−Air Batteries. *ACS Nano* **2013**, *7*, 3532−3539.
(40) Riaz, A.; Jung, K.-N.; Chang, W.; Lee, S.-B.; Lim, T.-H.; Park, S.-J.; Song, R.-H.; Yoon, S.; Shin, K.-H.; Lee, J.-W. Carbon-Free Cobalt Oxide Cathodes with Tunable Nanoarchitectures for Rechargeable Lithium−Oxygen Batteries. *Chem. Commun.* **2013**, *49*, 5984−5986.
(41) Lim, H.-D.; Park, K.-Y.; Song, H.; Jang, E. Y.; Gwon, H.; Kim, J.; Kim, Y. H.; Lima, M. D.; Robles, R. O.; Lepró, X.; Baughman, R. H.; Kang, K. Enhanced Power and Rechargeability of a Li−O_2 Battery Based on a Hierarchical-Fibril CNT Electrode. *Adv. Mater.* **2013**, *25*, 1348−1352.
(42) Nasybulin, E.; Xu, W.; Engelhard, M. H.; Li, X. S.; Gu, M.; Hu, D.; Zhang, J.-G. Electrocatalytic Properties of Poly(3,4-ethylenedioxythiophene) (PEDOT) in Li−O_2 Battery. *Electrochem. Commun.* **2013**, *29*, 63−66.
(43) Qin, Y.; Lu, J.; Du, P.; Chen, Z.; Ren, Y.; Wu, T.; Miller, J. T.; Wen, J.; Miller, D. J.; Zhang, Z.; Amine, K. In Situ Fabrication of Porous-Carbon-Supported α-MnO_2 Nanorods at Room Temperature: Application for Rechargeable Li−O_2 Batteries. *Energy Environ. Sci.* **2013**, *6*, 519−531.
(44) Oh, S. H.; Black, R.; Pomerantseva, E.; Lee, J.-H.; Nazar, L. F. Synthesis of a Metallic Mesoporous Pyrochlore as a Catalyst for Lithium−O_2 Batteries. *Nat. Chem.* **2012**, *4*, 1004−1010.